This article can be cited as A. Widyotriatmo, C. Maharnani and Suprijanto, Rehabilitation Procedure and Performance Measurement using Mechanical Rotary Impedance Actuator, International Journal of Artificial Intelligence, vol. 18, no. 1, pp. 218-236, 2020.

Rehabilitation Procedure and Performance Measurement using Mechanical Rotary Impedance Actuator

Augie Widyotriatmo, **Cahyoni Maharnani**, **Suprijanto**

Instrumentation and Control, Faculty of Industrial Technology, Institut Teknologi Bandung
Ganesa 10, Bandung (Indonesia);
Emails: augie@tf.itb.ac.id, cahyoni_m@yahoo.co.id, supri@tf.itb.ac.id

ABSTRACT

This paper proposes a procedure and metrics for performance assessment in limb rehabilitation using a mechanical rotary impedance actuator. One joint mechanical rotary actuator with a force sensor at the end effector is used as a prototype for rehabilitation of flexion movement of the arm. A trajectory for rehabilitation is developed consisting of two parameters which are the time of completion and the achievable range of motion (ROM). An impedance control is developed using free-regressor adaptive control, producing interaction force between the actuator and the patient. Based on patient's condition, the clinician can adjust the impedance setting of the rotary joint so that the arm rehabilitation actuator assists the patient only as much as needed. By setting the parameters of impedance and the rehabilitation trajectory, the patient follows a training procedure as in the active mode in which the impedance of the rotary joint is adjustable. In the proposed procedure, the patient is asked to follow the generated rehabilitation trajectory. The metrics are developed containing the motor function which is how close the patient can follow the rehabilitation trajectory, the maximum ROM a patient can achieve, and the strength index which is the maximum force that a patient can provide. Those metrics are calculated as the training procedure goes on. Ten healthy subjects perform the training procedure and the metrics show consistent results. Accordingly, the proposed metrics are potentially able to classify the ability of the patients and therefore can be used for monitoring the progress of a patient during the rehabilitation.

Keywords: Rehabilitation robot, trajectory generation, control, nonlinear compensation, proportional-integral.

Mathematics Subject Classification: 70E17, 70E60, 93C40,93C95

Computing Classification System: I.2.9, I.4

1. INTRODUCTION

Rehabilitation robotics have been conducted to accelerate the recovery of limbs disabled patient. It has been known that robot-assisted therapy significantly improves the motor functions of a patient (Husemann, et al., 2007; Kwakkel, Kollen, & Krebs, 2008). The mechanics of upper limb rehabilitation therapy can be based on unilateral end-effector robot, exoskeleton robot (Lo & Xie, 2012), cable-driven (Knuth et al., 2016), bilateral end-effector robot (Sheng et al. 2016), and multi-robot end-effector robot (Tóth et al., 2004; Jackson et al., 2007). For the unilateral end-effector robot, the end effector holds the patient's hand or forearm at a point and produces force at that point. The

exoskeleton robot has a structure with joint axes that matches with the human upper limb. The cable-driven robot holds the patient's forearm and arm/elbow using ropes with adjustable length so that particular motions such as shoulder and elbow flexion can be trained. The bilateral end-effector robot holds both hands and forearm of the patient and produces forces on the end effectors. The multi-robot end effector robot holds the forearm and elbow of a hand of the patient. All of these robots show the significant results depending on the use of training methods and also the use of control strategies.

The rehabilitation training based robotics can be classified into several modes. The passive mode is the rehabilitation mode where patient does not provide any movement during the rehabilitation; the robot performs position control and helps the patient to follow the predetermined trajectories through repeated training; by repeated intensive exercise, the motor function is improved and the muscle atrophy is reduced, but motivation of patient can be very low (Veneman et al., 2007; Saglia et al., 2009; Saglia et al., 2012; Hussain, Xie & Jamwal, 2013a; Hussain, Xie, Jamwal, 2013b; Jamwal et al, 2014). The action mode is the rehabilitation mode where patient should provide movement to the robot and the robot modifies the trajectories or assistance force; since the trajectory is determined by the patient, the initiative motivation can be increased (Veneman et al., 2007; Hussain, Xie, Jamwal, 2013a; Hussain, Xie, Jamwal, 2013b; Jamwal et al, 2014). The active-assist-mode is the rehabilitation mode where the patient moves the limb without assistance at the first time, and then the robot helps after the patient is no longer capable; this mode can improve the motivation of the patient since the patient may avoid the feelings of frustration (Veneman et al., 2007; Saglia et al., 2009; Pittaccio & Viscuso, 2011; Saglia et al., 2012). The active-resist-mode is the rehabilitation mode where the robot provides resistive force as the patient moves the limb; this mode is suitable for a patient that has highly recovered (Veneman et al., 2007; Saglia et al., 2009; Pittaccio & Viscuso, 2011; Saglia et al., 2012). The bimanual-mode is the rehabilitation mode in which the robot performs a mirror-image movement that is done by manual therapy; this mode is developed by the view of clinicians (Lum, Burgar, & Shor, 2004; Komada et al., 2009; Akdogan & Adli, 2011).

Several control functions for rehabilitation robotics have been proposed in relation to the training modes. The position control is the control that is implemented to track the predetermined position; this control method is used for early rehabilitation to provide repetitive training in passive mode (Emken et al., 2008; Vallery et al. 2009; Duschau-Wicke et al., 2010; Saglia et al., 2012; Hussain et al., 2013a; Jamwal et al., 2014; Pittacio & Viscuso, 2014). The force control is the control that is applied to perform position control and, at the same time, to track the desired force; this can be done by dividing the control scheme into an independent position control loop and a force control loop; the robot provides motion to track trajectory and also maintains desired force (Deutsch et al., 2001; Bernhardt et al., 2005; Ju et al., 2005; Simon et al., 2007; Duschau-Wicke et al., 2010). The impedance control is the control that can regulate the dynamic relationship between robot position and contact force; the impedance can be tuned to make the robot compliant, flexible, and adaptable to the needs of patient; most development of rehabilitation robotics nowadays uses this control strategy (Emken & Reinkensmeyer, 2005; Agrawal et al., 2007; Veneman et al., 2007; Duschau-Wicke et al., 2010; Hussain et al., 2013b; Koopman et al., 2013). Electromyogram (EMG)-based control is the control that utilizes EMG signals as the feedback in controlling the robot; this method allows interaction between

the patient and the robot through the information gathered from EMG signals (Krebs et al., 2003; Fleischer et al., 2006; Kiguchi et al., 2008; Song et al., 2008; Song et al., 2013; Lenzi et al., 2012; Yin et al., 2012; Fan & Yin, 2013). The assist-as-needed control is the control which enables the robot to adapt in assisting the force or impedance when the patient shows a better movement ability; this kind of control uses artificial intelligent methods that can adapt to the patient's need and assist the patient only as much as needed (Riener et al., 2005; Riener, Luenenberger, & Colombo, 2006; Wolbrecht, et al. 2008; Duschau-Wicke et al., 2010; Fleerkotte et al. 2014). Other methods may be used such as evolutionary computing (Odugawa, Tiwari, & Roy, 2005), iterative feedback using fuzzy control systems (Preitl et al., 2006), dynamic neural network (Garcia et al., 2011), and using optimization methods such as in (Shams et al., 2017).

The recovery analyses that are used for measuring the improvement of a patient are Fugl-Meyer arm motor score (FMA) (Volpe, et al., 2000) and functional independence measure (FIM) (Fasoli et al., 2004). The instruments are based on the patient function assessment where the area includes activities of daily living, functional mobility, etc. (Kwakkel, Kollen, & Krebs, 2008). Other performance assessment methods for assistance is metabolic cost, biomechanical analysis, muscle activity (Huo, Mohammed, Moreno, Amirat, 2016). The metabolic cost is the comparison of metabolic energy expenditure, calculated from the oxygen consumption, carbon dioxide production, and the urinary nitrogen excretion, while moving the limbs with and without the robot's assistance. The biomechanical function analysis includes the kinematic variables, temporal–spatial variables, physiological cost variables, and others related to the movement function. The muscle activity analysis is obtained by assessing the muscle's activation levels depending on the assistance performance.

Online assessment or measurement is needed to obtain the improvement of the patient during the therapy with the quantitative measurement based on the performance of the patient. The performance assessment during rehabilitation is also important for the clinician and the patient. A patient would learn to correct from the experiencing previous errors. Through the assessment, the clinician can adjust some parameters (such as impedance and force) and can set the targets of the training. Husemann et al. (2007) used functional ambulation classification (FAC) (Holden et al., 1984; Holden et al., 1986) and muscle power determined by Motricity Index (MI) (Demeuriss, Demol, Robaye, 1980; Gregson et al., 2000), and Barthel Index (BI) (Mahoney & Barthel, 1965). Blaya and Herr (2004) used the speed and force as the biomechanical variables for robot-assist limb. Kawamoto and Sankai (2005) utilizes trajectory of joints, torque, and also EMG for determining the performance of a patient using gait exoskeleton.

In this paper, a prototype of rotary motor variable impedance designed for flexion movement rehabilitation of elbow is utilized. A smooth trajectory for rehabilitation is designed where its parameters, the achievable ROM and the time to accomplish of the trajectory, are adjustable; it is called a rehabilitation trajectory. The clinician sets the impedance of the arm rehabilitation actuator and the patient is asked to follow a rehabilitation trajectory. The impedance control is designed so that the motor provides assistance according to the impedance setting. Three metrics of performance on a patient using arm rehabilitation actuator are proposed. First metric is the motor function performance

of a patient which is conducted with the error criteria between the angular trajectory of the patient movement and the predetermined rehabilitation trajectory. The second metric is the maximum ROM of the patient which is directly measured by the rotary encoder. The third metric is the measured maximum force measured by the end effector force sensor. The metrics are tested to ten (10) healthy subjects and the consistency of the metrics is analyzed.

2. ARM REHABILITATION ACTUATOR

2.1. The Structure and Model of the Arm Rehabilitation Actuator

The arm rehabilitation actuator is configured as two links with one joint actuated by a DC motor (Fig. 1). The elbow of the patient is placed at the joint, the arm and shoulder are strapped on the Link #1 and Link #2, respectively. The DC motor provides the torque to the joint. A force sensor is attached to the tip of the Link #2 to measure the force given by the patient. An absolute encoder is attached to measure the angle of the joint.

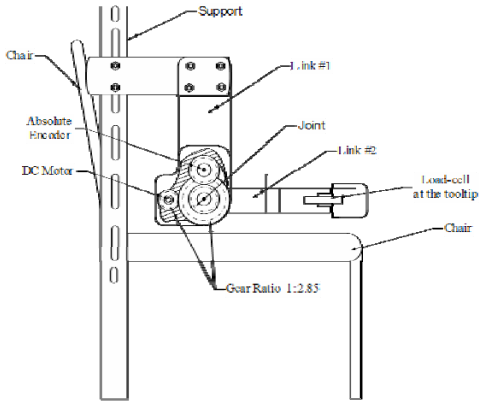

Fig. 1. The prototype of arm rehabilitation actuator.

The model of arm rehabilitation actuator is illustrated in Fig. 2. The DC motor produces torque τ_{m} to manipulate the angular displacement. The length of Link #2 is $2l$ and its weight is G. The external force f_{e} is measured by the load cell. The mathematical model is derived using the Lagrangian function L:

$$L = K - P = (1/2) I_{\mathrm{R}} (\dot{\theta})^2 - Gl\cos\theta \,, \tag{1}$$

where $K = (1/2) I_R \left(\dot{\theta}\right)^2$ is the kinetic energy, I_{R} is the inertia of Link #2 at the joint, $\dot{\theta}$ is the angular velocity, and $P = Gl\cos\theta$ is the potential energy of the system. The dynamic of the arm rehabilitation actuator is derived as follows:

$$\psi = \frac{d}{dt}\left(\frac{\partial L}{\partial \dot{\theta}}\right) - \frac{\partial L}{\partial \theta}, \tag{2}$$

where ψ is the resultant torque working on the system consisted of torque provided by the motor τ_{m}, the external torque given by the force of patient f_{e}, and the friction torque represented by the positive friction coefficient B_{R} and the angular velocity $\dot{\theta}$. The resultant torque ψ is obtained as follows:

$$\psi = \tau_{\mathrm{m}} - B_{\mathrm{R}}\dot{\theta} + 2lf_{\mathrm{e}} \,. \tag{3}$$

By substituting (3) into (2) and solving the partial derivative terms in (2), the dynamic model of the arm rehabilitation actuator is obtained as

$$I_{\mathrm{R}}\ \ddot{\theta} + B_{\mathrm{R}}\dot{\theta} + Gl\sin\theta = \tau_{\mathrm{m}} + 2lf_{\mathrm{e}} \,, \tag{4}$$

where $\ddot{\theta}$ is the angular acceleration of the joint.

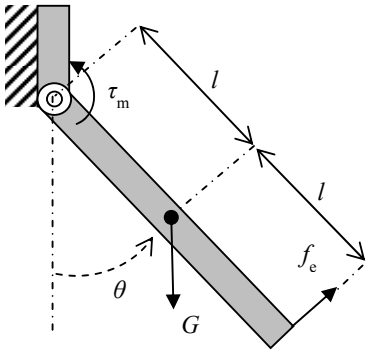

Fig. 2. The schematic model of arm rehabilitation actuator.

2.2. Rehabilitation trajectories and impedance scheme

Trajectory for limb rehabilitation should be synchronized with the ability of the patient (Vallery et al., 2009). In this paper, a function of rehabilitation trajectory $\theta_d(t)$ is designed as a smooth function in which two parameters, the time of completion and the achievable range of motion (ROM), are adjustable. One function candidate is

$$\theta_d(t) = \begin{cases} \theta_{ach}\left(1+\sin\left(\frac{\pi t}{T_c}-\frac{\pi}{2}\right)\right), & t < T_c, \\ \theta_{ach}, & t \geq T_c, \end{cases} \tag{5}$$

where θ_{ach} is the achievable ROM provided to the joint of the patient and T_c is the time period for completing the trajectory. The achievable ROM θ_{ach} and the time period for completing the trajectory T_c are adjustable by a clinician according to the capability of the patients. Fig. 3 shows two trajectories in which, for both trajectories, the θ_{ach} is $2\pi/3$, and the time periods for completion are 5s ad 10s.

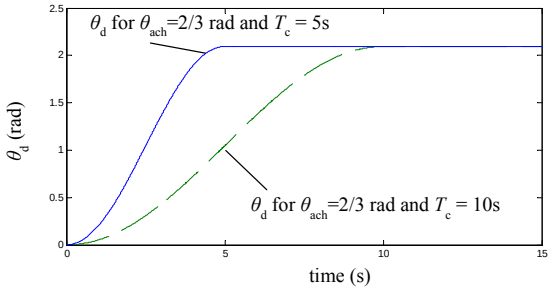

Fig. 3. Rehabilitation trajectory θ_d using equation (5) with $\theta_{ach} = 2\pi/3$ and the time for completion is T_c = 5s (solid) and T_c = 10s (dashed).

2.3. Free-Regressor Adaptive Control

The motor provides the torque τ_m that is needed to achieve the following impedance characteristic

$$\left(J\left(\ddot{\theta}_i - \ddot{\theta}_d\right) + O\left(\dot{\theta}_i - \dot{\theta}_d\right) + Q\left(\theta_i - \theta_d\right)\right) = \tau_d \tag{6}$$

where θ_{i} is the generated impedance trajectory, τ_{d} is the as needed torque given to the actuator, J, O, and Q are the impedance parameters related to the desired moment of inertia, damping, and stiffness coefficients, respectively. The choice of impedance parameters specify the impedance characteristic of the mechanical arm, e.g., high or low impedance. For a system where the parameters I_{R}, B_{R}, G are known, the τ_{m} can simply be designed as

$$\tau_{\mathrm{m}} = I_{\mathrm{R}}\ddot{\theta} + B_{\mathrm{R}}\dot{\theta} + Gl\sin\theta - 2lf_{\mathrm{e}} + \tau_{\mathrm{d}} - \left(J\left(\ddot{\theta}_{\mathrm{i}} - \ddot{\theta}_{\mathrm{d}}\right) + O\left(\dot{\theta}_{\mathrm{i}} - \dot{\theta}_{\mathrm{d}}\right) + Q\left(\theta_{\mathrm{i}} - \theta_{\mathrm{d}}\right)\right). \quad (7)$$

Substituting (7) into (4) yields (6). This control law in (7) cannot be directly applied to the system since the values of inertia I_{R}, the friction coefficient B_{R}, and the gravitational term G cannot be determined accurately. Therefore, a free-regressor adaptive control algorithm is designed to determine the control input τ_{m}.

The adaptive control is established to design the torque motor control so that the impedance characteristics of (6) is achieved with the adaptability to the unknown parameters of I_{R}, B_{R}, and G. The scheme of free-regressor adaptive control estimates the values of unknown parameters I_{R}, B_{R}, and G without a regressor-function. An impedance trajectory is generated using the desired rehabilitation trajectory as in (6).

Let e be the error between the impedance trajectory θ_{i} and the angular angle of the actuator θ, which is

$$e = \theta - \theta_i. \quad (8)$$

Variables v and s are defined as follows:

$$v = \dot{\theta}_i - ce, \quad (9)$$

$$s = \dot{e} + ce. \quad (10)$$

where c is a positive constant. Using (8)-(10), (4) becomes

$$I_{\mathrm{R}}\,\dot{s} + B_{\mathrm{R}}s + Gl\sin\theta + I_{\mathrm{R}}\dot{v} + B_{\mathrm{R}}v = \tau_{\mathrm{m}} + 2lf_{\mathrm{e}}. \quad (11)$$

Let $\tilde{I}_R$, $\tilde{B}_R$, and $\tilde{G}$ be the difference between the true values of I_{R}, B_{R}, and G, respectively, and their estimates $\hat{I}_R$, $\hat{B}_R$, and $\hat{G}$, respectively, which are:

$$\tilde{I}_R = I_R - \hat{I}_R, \quad (12)$$

$$\tilde{B}_R = B_R - \hat{B}_R, \quad (13)$$

$$\tilde{G} = G - \hat{G}. \quad (14)$$

The control and adaptive laws are formulated using a Lyapunov function candidate V as

$$V\left(s, \tilde{I}_R, \tilde{B}_R, \tilde{G}\right) = \frac{1}{2}I_R\,s^2 + \frac{1}{2}\tilde{I}_R^2 + \frac{1}{2}\tilde{B}_R^2 + \frac{1}{2}\tilde{G}^2, \quad (15)$$

where V is positive definite. The time derivative of the Lyapunov function (15) is

$$\dot{V}\left(s, \tilde{I}_R, \tilde{B}_R, \tilde{G}\right) = I_R\,s\dot{s} + \tilde{I}_R\dot{\tilde{I}}_R + \tilde{B}_R\dot{\tilde{B}}_R + \tilde{G}\dot{\tilde{G}}. \quad (16)$$

Using (11)-(14), (16) becomes

$$\dot{V}\left(s,\tilde{I}_R,\tilde{B}_R,\tilde{G}\right)=-B_{\mathrm{R}}s^2-I_{\mathrm{R}}\dot{v}s-Gl\left(s\sin\theta\right)+\left(\tau_{\mathrm{m}}+2lf_{\mathrm{e}}\right)s-B_{\mathrm{R}}vs-\tilde{I}_R\dot{\hat{I}}_R-\tilde{B}_R\dot{\hat{B}}_R-\tilde{G}\dot{\hat{G}}. \tag{17}$$

The control law τ_{m} is designed as

$$\tau_m=\hat{I}_R\,\dot{v}+\hat{B}_R v+\hat{G}\sin\theta-2lf_e-Ks\ , \tag{18}$$

where K is a positive gain. By substituting (18) into (17), we obtain

$$\dot{V}\left(s,\tilde{I}_R,\tilde{B}_R,\tilde{G}\right)=-(B_{\mathrm{R}}+K)s^2-\tilde{I}_{\mathrm{R}}\dot{v}s-\tilde{G}l\left(s\sin\theta\right)-\tilde{B}_{\mathrm{R}}vs-\tilde{I}_R\dot{\hat{I}}_R-\tilde{B}_R\dot{\hat{B}}_R-\tilde{G}\dot{\hat{G}}. \tag{19}$$

The adaptive laws are designed as follows:

$$\dot{\hat{I}}_{\mathrm{R}}=-\left(\dot{v}s\right), \tag{20}$$

$$\dot{\hat{B}}_{\mathrm{R}}=-\left(vs\right), \tag{21}$$

$$\dot{\hat{G}}=-l\left(s\sin\theta\right). \tag{22}$$

Using (20)-(22), (19) becomes

$$\dot{V}\left(s,\tilde{I}_R,\tilde{B}_R,\tilde{G}\right)=-(B_{\mathrm{R}}+K)s^2. \tag{23}$$

Theorem. Let the dynamics of arm actuator be in (4). Applying the control law in (18) and the adaptive laws (21)-(23) to the system (4), the origin of the angular error e is asymptotically stable.

Proof. By the analysis of the Lyapunov function (15), it is obtained in (23) that, using the control law (18) the adaptive laws (20)-(22), the time derivative of the Lyapunov function $\dot{V}\left(s,\tilde{I}_R,\tilde{B}_R,\tilde{G}\right)\le 0$ is negative semi-definite. From (23), it is concluded that $s(t)\to 0$ as $t\to\infty$. From (10), $\dot{e}+ce=0$ as $t\to\infty$, and since c is a positive constant, then $e(t)\to 0$ as $t\to\infty$. □

By this theorem, applying the control law (18) and adaptive laws (20)-(22) assure that the angular joint θ converges to the angular impedance θ_{i}. The schematic of impedance scheme for arm rehabilitation actuator is described in Fig. 4. The controller parameter K is determined by minimizing the error trajectory subject to the allowable gain with respect to the sampling frequency.

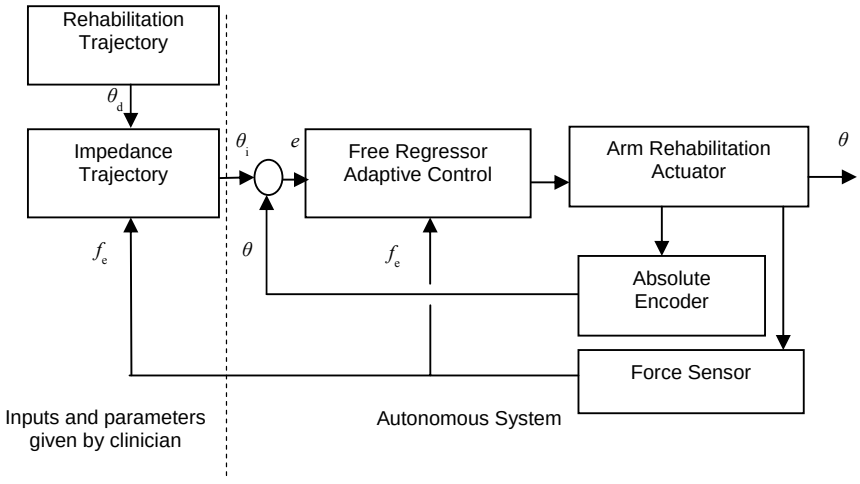

Fig. 4. Impedance scheme for the arm rehabilitation actuator.

3. IMPLEMENTATION OF ARM REHABILITATION ACTUATOR

3.1. Experimental setup and training procedure

Fig. 5 shows the experimental setup and the graphical user interface (GUI) that is used by the subject to see the rehabilitation trajectory. The GUI shows rehabilitation trajectory, the angular trajectory, the motor function metrics, and the measured force in real-time. The training starts by setting the parameters of rehabilitation trajectory, including the time of completion and the achievable ROM, and those of impedance, including I_{R} , B_{R} , G and τ_{d} . After the patient is connected to the arm rehabilitation actuator, the patient is asked to follow the rehabilitation trajectory shown on the monitor. When the training starts, the rehabilitation performance is measured, in which the metrics are described in Section 4. The training procedure is depicted in Fig. 6.

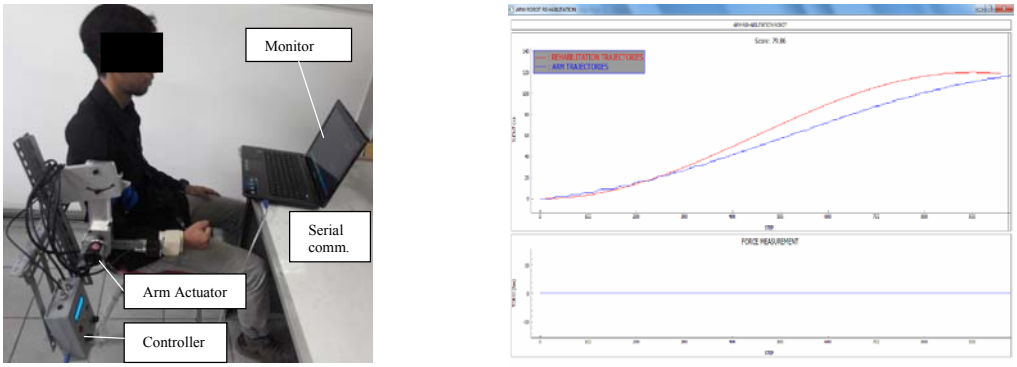

(a) (b)

Fig. 5. One healthy subject performs a training following rehabilitation trajectory. (a) The experimental setup. (b) The monitor shows GUI consisting the real-time rehabilitation trajectory, the angular trajectory, the motor function metrics, and the measured force.

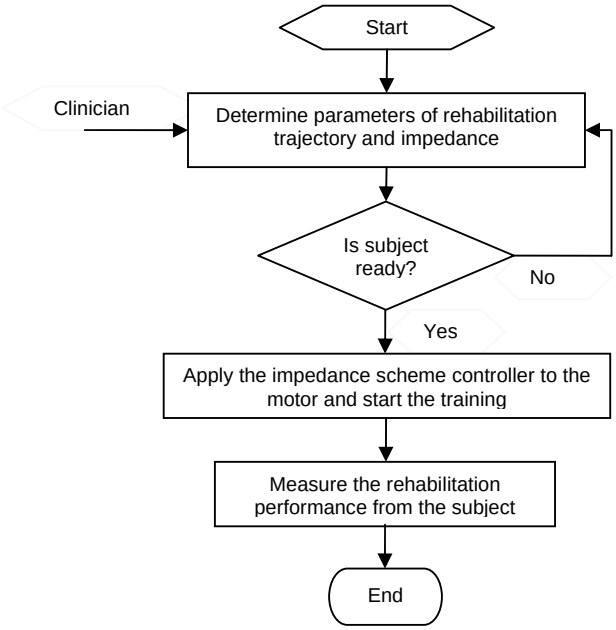

Fig. 6. The training procedure.

3.2. Impedance settings without subject movement

The impedance control plays a significant role in the scheme of arm rehabilitation. The objective is to maintain the angular joint to follow the given impedance behavior. This section shows the performance of the designed impedance control performs in two scenarios, which are the high and low setting impedance. In this experiments, the subject does not provide the movement. The time for completion is set to 20 s. The achievable ROM θ_{ach} is set to 2.09 rad (or 120°). The motor used has a maximum power of 1.2 N·m. The parameters used to generate the impedance trajectories are $J = 1$, $O = 4$, and $Q = 1$ and 4. Both $Q = 1$ and $Q = 4$ perform no oscillation impedance trajectory since the poles lie on negative real axis. $Q = 1$ provides the impedance behavior to have low impedance and $Q = 4$ provides high impedance. The weight of patient's and robot's arm G in the experiment is 1.5 N. τ_{d} is set so that the weight of patient's and robot's arm is compensated. The controller parameter is set at K = 100 N·m/s^2. Fig. 7 shows the rehabilitation trajectory, impedance trajectories with low and high impedances, and the resulted angular joints. The impedance trajectories are followed by the individual angular joints.

Fig. 8 shows that the motor provides different assistive powers for different impedance settings. At the high impedance setting Q = 4, the motor provides high assistive power, and at the low impedance setting Q = 1, the motor provides low assistive power. Fig. 9 shows the force measured at the tip of Link #2 during the training. When the high impedance is set Q = 4, the measured force is lower than that when the low impedance is set Q = 1. This happens because, when the high impedance is set, the link provides more torque to the patient's arm, and as a result, the patient's arm opposes reaction to the link, and the link receives more force as captured by the force sensor.

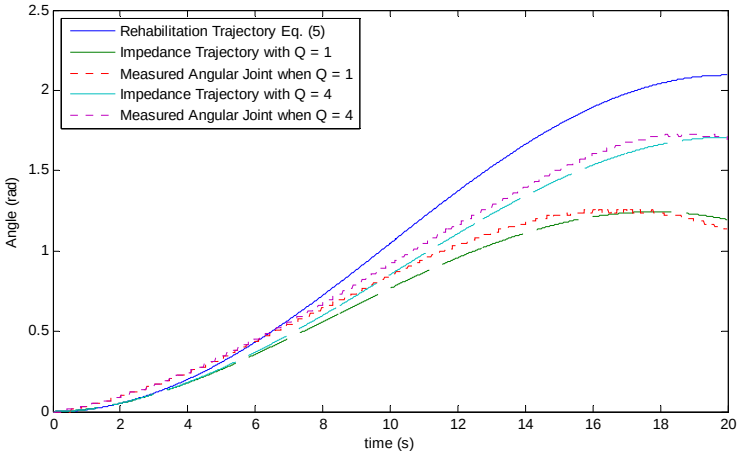

Fig. 7. The angle of rehabilitation trajectory, impedance trajectories, and the angular joint.

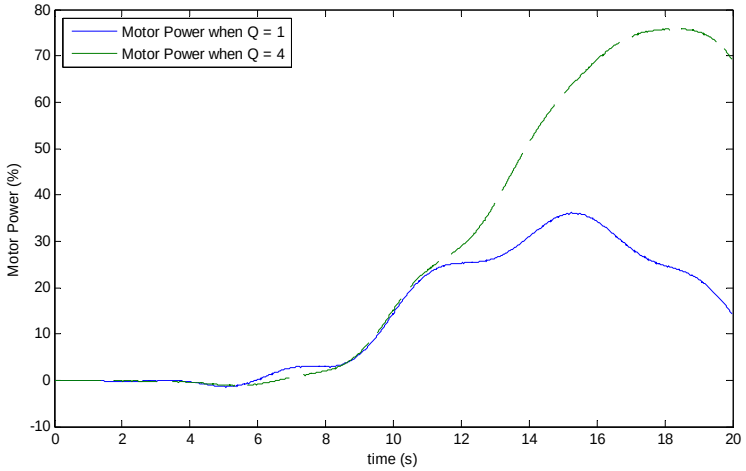

Fig. 8. The motor power provided to the joint when the low impedance is set $Q = 1$ (solid) and when the high impedance is set $Q = 4$ (dashed).

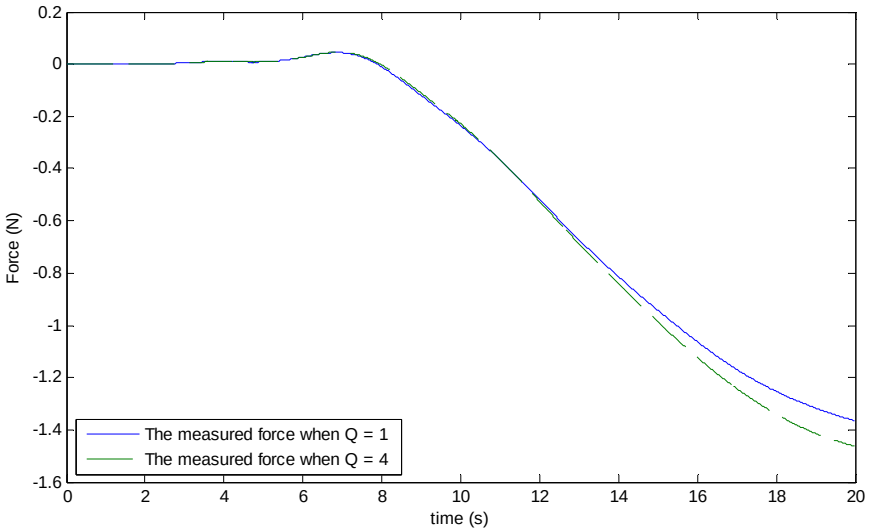

Fig. 9. The measured force at the tip of Link #2 when the when low impedance is set $Q = 1$ (solid) and when the high impedance is set $Q = 4$ (dashed).

3.3. Low impedance setting with subject movement

In this experiments, the interaction between the arm rehabilitation actuator and the patient is investigated. By setting the parameters to low impedance, the arm rehabilitation robot complies with the movement of the patient. The performance parameterization of the patient is developed based on the ability of the patient in following the desired rehabilitation trajectory designed in equation (5). The stiffness *Q* is set to 1. The time for completion is set to 20 s. The achievable ROM θ_{ach} is set to 2.09 rad (or 120°). τ_{d} is set so that the weight of patient's and robot's arm is compensated.

The subject used in this experiment is a healthy person. At first, the subject is asked to relax and to not follow the movement of the arm rehabilitation robot. Next, the subject is asked to follow the

rehabilitation trajectory displayed on the monitor. Fig. 10 shows rehabilitation trajectory and the angular joint when the subject follows and does not follow the rehabilitation trajectory.

Fig. 11 shows the percentage of power given by the motor in both cases. The motor provides less power when the subject follows the rehabilitation trajectory and more power when the subject follows the rehabilitation trajectory due to the load that is given to the motor. The forces measured at the tooltip of the link for the individual cases are shown in Fig. 12.

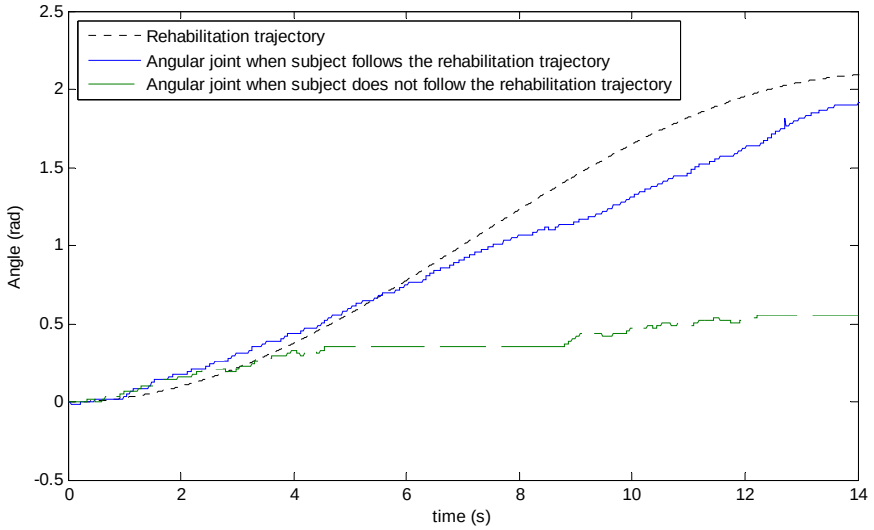

Fig. 10. The trajectories of designed rehabilitation trajectory (dot), the measured angular joints when subject follows the rehabilitation trajectory (solid) and when the subject does not follow the rehabilitation trajectory (dashed). The angular joint when subject follows the rehabilitation trajectory shows the less error (between the rehabilitation trajectory and the angular joint) compared to that when the subject does not follow the rehabilitation trajectory.

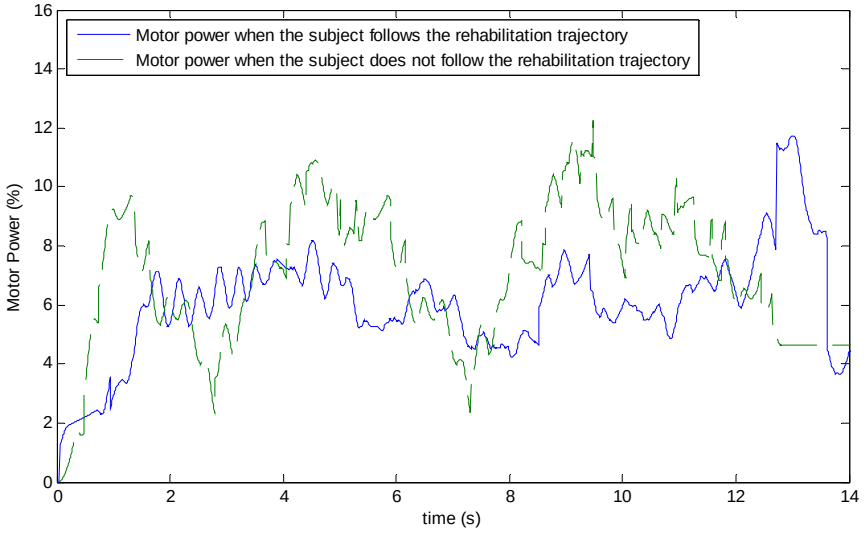

Fig. 11. The motor power when the subject follows the rehabilitation trajectory (solid) is lesser than that when the subject does not follow the rehabilitation trajectory (dashed).

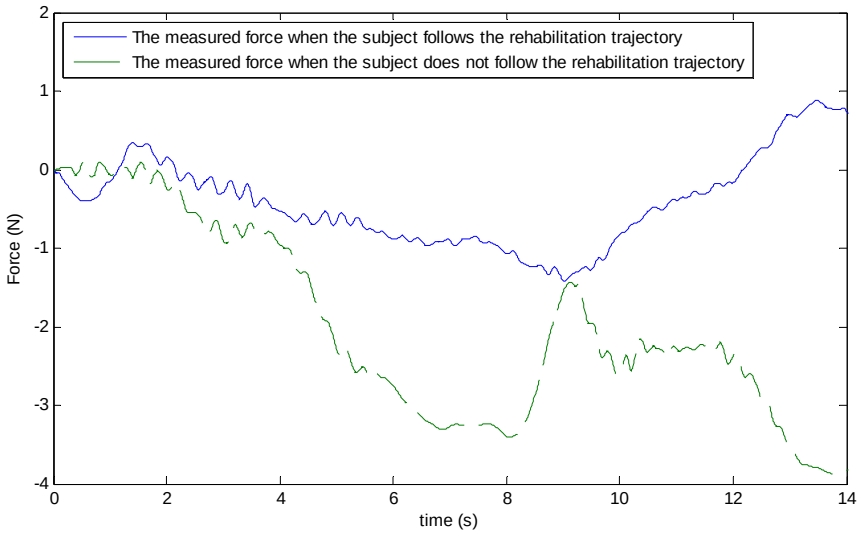

Fig. 12. The forces measured by the load cell when the subject follows the rehabilitation trajectory (solid) and when the subject does not follow the rehabilitation trajectory (dashed). When the subject does not follow the rehabilitation trajectory, the link #2 encounters more negative force due to the weight of the subject's arm.

4. PERFORMANCE MEASUREMENTS

4.1. The proposed performance metrics

In the rehabilitation training activity, the first proposed metric is the ability of the patient to follow the rehabilitation trajectory given by the clinician. The second metric is the joint performance represented by the maximum range of motion (ROM). The third metric is the strength of the patient represented by the maximum of force. The metrics are subjected to the parameters of rehabilitation trajectories and the impedance of the mechanical rotary actuator set by the clinician.

The proposed motor function index $P \in [0, 1]$ for rotary flexion movement of a subject is defined by the following:

$$P = 1 - \frac{\left| \sum_{k}^{N} \theta_{\mathrm{d}} - \sum_{k}^{N} \theta \right|}{\sum_{k}^{N} \theta_{\mathrm{d}}}, \tag{24}$$

where $k = 1, 2, \ldots, N$ represents the sequence corresponding to the sampling time T; $\theta(kT)$ is the angle θ at time kT. The dimensionless motor function index (24) indicates that if the trajectory $\theta(t)$ is the same as the rehabilitation trajectory $\theta_{\mathrm{d}}(t)$, the maximum performance 1 is achieved. This metric indicates how close the subject can follow the desired trajectory. When the training is done repeatedly, the distribution of the motor function index shows the endurance which is the ability to sustain or repeat the muscular activity over time.

The maximum range of motion $\theta_{\max \mathrm{ROM}}$ of a patient is conducted through the following metric:

$$\theta_{\max \mathrm{ROM}} = \max_k \theta(k) \text{ [rad].} \quad (25)$$

This metric indicates the maximum range of motion of a subject during the rehabilitation training. The maximum range of motion describes the flexibility of the joint.

The proposed strength index *S* for the rotary flexion movement of a subject is defined by the following:

$$S = \max_k f_{\mathrm{e}}(k) \text{ [N].} \quad (26)$$

The index *S* indicates the maximum force that can be generated by the subject during the rehabilitation training. The maximum force describes the strength capability of the patient.

The work index *W* during the training is calculated as follows:

$$W = \sum_k^N f_e(k)\Delta\theta \text{ [J].} \quad (27)$$

This represents the total work that is done by a subject during the training.

4.2. Implementation and analysis of the performance metrics

The experiments are conducted by using ten healthy subjects. Each subject performs five experiments where the subjects are asked to follow the predefined rehabilitation trajectory. The rehabilitation trajectory parameters are set as follows: the time of completion for rehabilitation trajectory is 14 sec; the impedance is set at J = *1*, O = 4, Q = 1, and τ_{d} is set in such a way that the weight of the subject is compensated. All subjects have never been trained using the prototype.

The distribution of the individual subjects for motor function index P, the maximum ROM $\theta_{\max \mathrm{ROM}}$, the strength index S , and the work performance index W are shown in Figs 13-16, respectively. The central mark inside the box (with red ink) is the median, the edges of the box are the 25th and 75th percentiles, and the outer whiskers are the extreme data points. It can be seen that the healthy subjects can achieve high index in a consistent manner. The motor function index and the maximum ROM $\theta_{\max \mathrm{ROM}}$ have small variations among the experiments. The force and work performance indexes show many variations, however the minimum work that is obtained from the healthy subject still provides a value of 13 Joule.

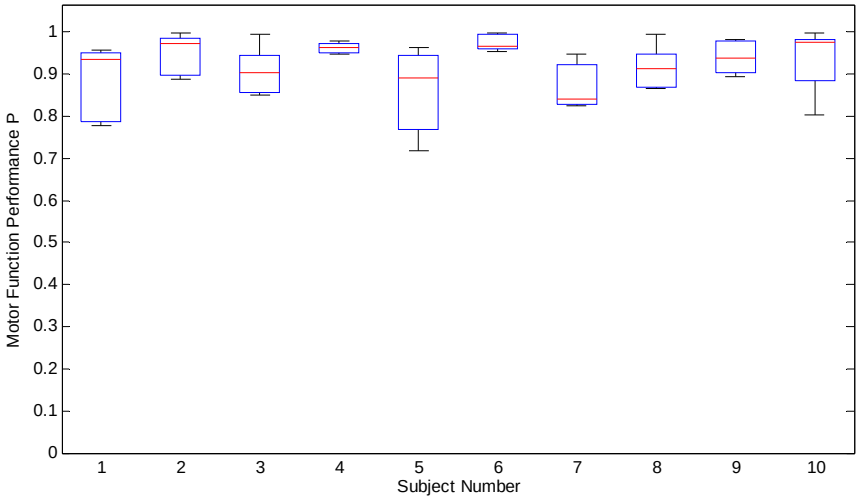

Fig. 13. The distribution of motor function index *P* obtained from the experiments of ten healthy subjects.

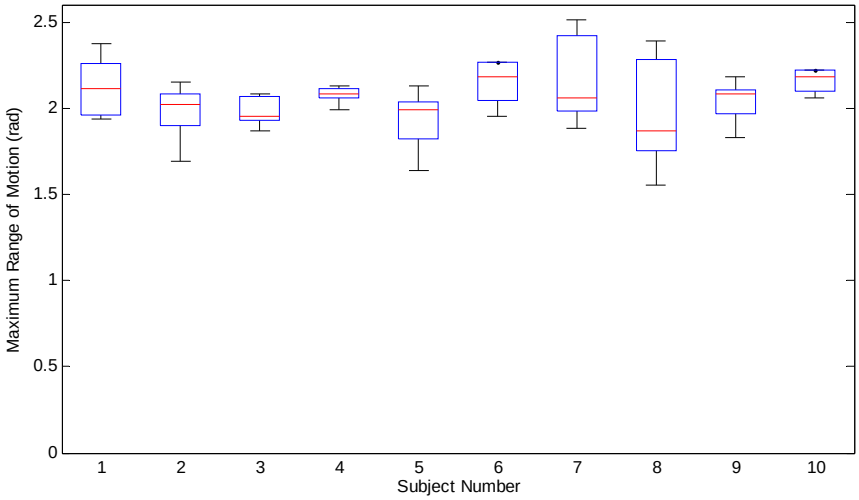

Fig. 14. The distribution of the maximum ROM $\theta_{\max \mathrm{ROM}}$ obtained from the experiments of ten healthy subjects.

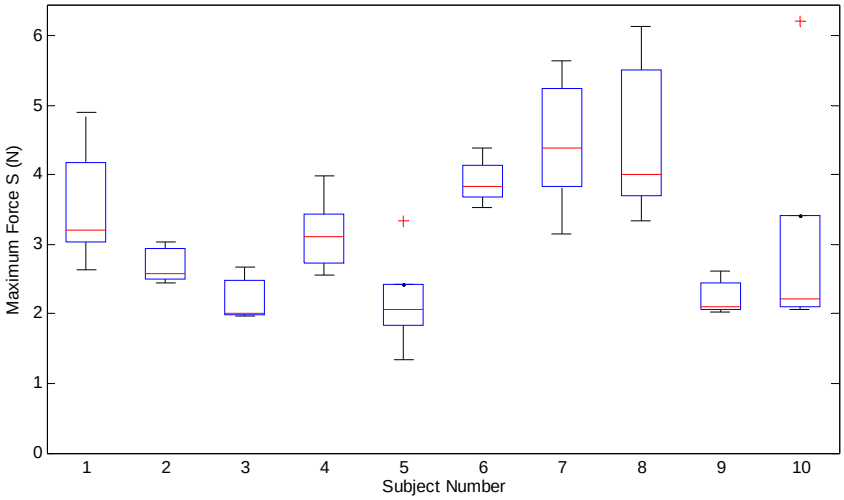

Fig. 15. The distribution of strength index *S* obtained from the experiments of ten healthy subjects. The + sign denotes the extreme values which is out of a distribution.

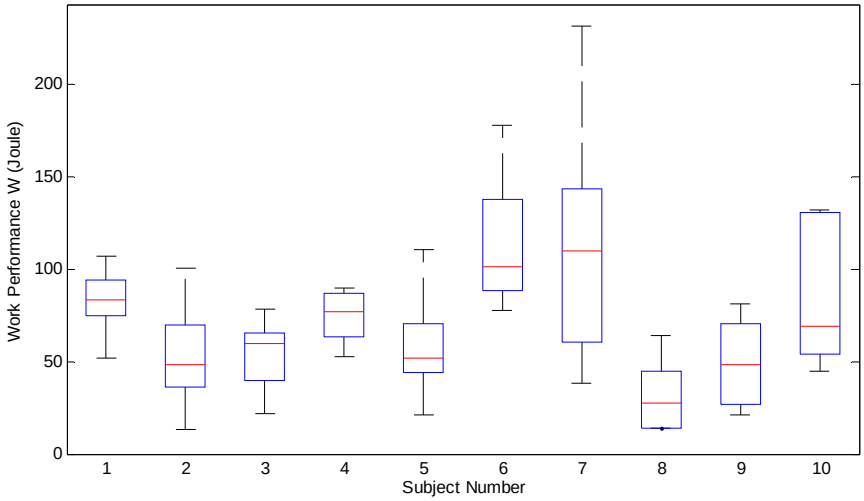

Fig. 16. The distribution of work performance obtained from the experiments of ten healthy subjects.

5. CONCLUSION

In this paper, the rehabilitation procedure and performance measurement for rehabilitation patient using arm rehabilitation actuator are proposed. The metrics include the motor function index which is how close a subject is able to follow a predesigned trajectory, the maximum range of motion which is how achievable range of motion of a subject, and the strength index which is the maximum force provided by the subject in a particular setting of impedance. The impedance setting of the rehabilitation actuator is adjustable to provide different force depending on the capability of the patient. The experiments of the metrics implementation to healthy subjects show that the metrics are potentially able to discriminate between the healthy subjects with the patients being in the physical rehabilitation. The metrics are potentially be used as progress measurement of a rehabilitation patient.

Future research directs the implementation of the proposed metrics to rehabilitation robot which has more degree of freedom, and the proposed metrics need to be conducted with the standard metrics that have been generally utilized by the clinicians.

REFERENCES

Agrawal, S. K., Banala, S. K., Fattah, A., Sangwan, V., Krishnamoorthy, V., Scholz, J. P., Hsu, W.-L. (2007). Assessment of motion of a swing leg and gait rehabilitation with a gravity balancing exoskeleton. *IEEE Transactions on Neural Systems and Rehabilitation Engineering*, 15, 410–420.

Akdogan, E., Adli, M. A. (2011). The design and control of a therapeutic exercise robot for lower limb rehabilitation: physiotherabot. *Mechatronics*, 21, 509–522.

Blaya, J. A., Herr, H. (2004). Adaptive control of a variable-impedance ankle foot orthosis to assist drop-foot gait. *IEEE Transactions on Neural Systems and Rehabilitation Engineering*, 12 (1), 24–31.

Bernhardt, M., Frey, M., Colombo, G., Riener, R. (2005). Hybrid force-position control yields cooperative behaviour of the rehabilitation robot LOKOMAT. *Proceedings of the 2005 IEEE 9th International Conference on Rehabilitation Robotics*, 536–539.

Demeuriss, G., Demol, O., Robaye, E. (1980). Motor evaluation in vascular hemiplegia. *European Neurology*, 19, 382-389.

Deutsch, J. E., Latonio,, J., Burdea, G. C., Boian, R. (2001). Post-stroke rehabilitation with the Rutgers Ankle system: a case study. *Presence: Teleoperators and Virtual Environments*. 10, 416–430.

Duschau-Wicke, A., von Zitzewitz, J., Caprez, A., Luenenburger, L., Riener, R. (2010). Path control: a method for patient-cooperative robot-aided gait rehabilitation. *IEEE Transactions on Neural Systems and Rehabilitation Engineering*, 18, 38–48.

Emken, J. L., Reinkensmeyer, D. J. (2005) Robot-enhanced motor learning: accelerating internal model formation during locomotion by transient dynamic amplification. *IEEE Transactions on Neural Systems and Rehabilitation Engineering*, 13, 33-39.

Emken, J. L., Harkema, S. J., Beres-Jones, J. A., Ferreira, C. K., Reinkensmeyer, D. J. (2008). Feasibility of manual teach-and-replay and continuous impedance shaping for robotic locomotor training following spinal cord injury. *IEEE Transactions on Biomedical Engineering*, 55, 322-334.

Fan, Y., Yin, Y. (2013). Active and progressive exoskeleton rehabilitation using multisource information fusion from sEMG and force-position EPP. *IEEE Transactions on Biomedical Engineering*, 60(12), 3314 - 3321.

Fasoli S. E., Krebs H. I., Ferraro, M., Hogan, N, Volpe, B. T. (2004). Does shorter rehabilitation limit potential recovery poststroke? *Neurorehabilitation and Neural Repair*, 18, 88-94.

Fleerkotte, B. M., Koopman, B., Buurke, J. H., van Asseldonk, E. H. F., van der Kooij, H., Rietman, J. S. (2014). The effect of impedance-controlled robotic gait training on walking ability and quality in individuals with chronic incomplete spinal cord injury: an explorative study. *Journal of Neuroengineering and Rehabilitation*, 11.

Fleischer, C., Wege, A., Kondak, K., Hommel, G. (2006). Application of EMG signals for controlling exoskeleton robots. *Biomedizinische Technik*, 51, 314–319.

Garcia, A., Luviano-Juarez, A., Chairez, I., Poznyak, A., Poznyak, T. (2011). Projectional dynamic neural network identifier for chaotic systems: Application to Chua's circuit. *International Journal of Artificial Intelligence*, 6(S11), 1-18

Gregson, J. M., Leathley, M. J., Moore, P., Smith, T. L., Sharma, A. K., Watkins, C. (2000). Reliability of measurements of muscle tone and muscle power in stroke patients. *Age Ageing*. 29, 223-228.

Holden, M. K., Gill, K. M., Magiliozzi, M. R., Nathan, J., Piehl-Baker, L. (1984). Clinical gait assessment in the neurologically impaired. Reliability and meaningfulness. *Physical Therapy*, 1984, 64, 35-40.

Holden, M. K., Gill, K. M., Magliozzi, M. R. (1986). Gait assessment for neurologically impaired patients. *Physical Therapy*, 66, 1530-1539.

Huo, W., Mohammed, S., Moreno, J. C., Amirat, Y., (2016). Lower limb wearable robots for assistance and rehabilitation: A state of the art. *IEEE Systems Journal*, 10(3), 1068-1081.

Husemann, B., Müller, F., Krewer, C., Heller, S., Koenig, E. (2007). Effects of locomotion training with assistance of a robot-driven gait orthosis in hemiparetic patients after stroke. *Stroke*, 38(2), 349–354.

Hussain, S., Xie, S. Q., Jamwal, P. K. (2013a). Robust nonlinear control of an intrinsically compliant robotic gait training orthosis. *IEEE Transactions on Systems, Man, and Cybernetics*: Systems, 43, 655–665.

Hussain, S., Xie, S. Q., Jamwal, P. K. (2013b) Adaptive impedance control of a robotic orthosis for gait rehabilitation. *IEEE Transactions on Systems, Man, and Cybernetics* Part B: Cybernetics, 43, 1025–1034.

Jackson, A., Holt, R., Culmer, P., Makower, S., Levesley, M., Richardson, R. (2007). Dual robot system for upper limb rehabilitation after stroke: the design process. *Proceedings of the Institute Mech Eng Part C: Journal of Mechanical Engineering and Science*, 221, 845–57.

Jamwal, P. K., Xie, S. Q., Hussain, S., Parsons, J. G. (2014). An adaptive wearable parallel robot for the treatment of ankle injuries. *IEEE/ASME Transactions on Mechatronics*, 19, 64–75.

Ju, M. S., Lin, C. C. K., Lin, D. H., Hwang, I. S., Chen, S. M. (2005). A rehabilitation robot with force position hybrid fuzzy controller: hybrid fuzzy control of rehabilitation robot. *IEEE Transactions on Neural Systems and Rehabilitation Engineering*, 13, 349–358.

Kawamoto, H., Sankai, Y. (2005). Power assist method based on phase sequence and muscle force condition for HAL. *Advanced Robotics*, 19(7), 717–734.

Kazerooni, H., Steger, R., Huang L. H. (2006). Hybrid control of the Berkeley lower extremity exoskeleton (BLEEX). *International Journal of Robotic Research*, 25, 561–573.

Kiguchi, K., Rahman, M. H., Sasaki, M., Teramoto, K. (2008). Development of a 3DOF mobile exoskeleton robot for human upper-limb motion assist. *Robotics and Autonomous Systems*, 56, 678–691.

Knuth, S., Passon, A., Dähne, F., Niedeggen, A., Schmehl, I., Schauer, T. (2016). Adaptive arm weight support using a cable-driven robotic system. *Proceedings of the 3rd International Conference on NeuroRehabilitation* (ICNR2016), October 18-21, 2016, Segovia, Spain.

Komada, S., Hashimoto, Y., Okuyama, N., Hisada, T., Hirai, J. (2009). Development of a biofeedback therapeutic-exercise-supporting manipulator. *IEEE Transactions on Industrial Electronics*, 2009, 56, 3914–3920.

Koopman, B., van Asseldonk E. H. F., van der Kooij, H. (2013). Selective control of gait subtasks in robotic gait training: foot clearance support in stroke survivors with a powered exoskeleton. *Journal of Neuroengineering Rehabilitation*, 10:3.

Krebs, H. I., Palazzolo, J. J., Dipietro, L., Volpe, B. T., Hogan, N. (2003). Rehabilitation robotics:performance-based progressive robot-assisted therapy. *Autonomous Robots*, 15, 7–20.

Kwakkel, G., Kollen, B. J., Krebs, H. I. (2008). Effects of robot-assisted therapy on upper limb recovery after stroke: A systematic review, *Neurorehabilitation and Neural Repair*, 22(2), 111-121.

Lenzi, T., De Rossi, S. M. M., Vitiello, N., Carrozza, M. C. (2012). Intention-based EMG control for powered exoskeletons. *IEEE Transactions on Biomedical Engineering*, 59, 2180–2190.

Lo, H. S., Xie, S. Q. (2012). Exoskeleton robots for upper-limb rehabilitation: State of the art and future prospects. *Medical Engineering Physics*, 34, 261-268.

Lum, P. S., Burgar, C. G., Shor, P. C. (2004). Evidence for improved muscle activation patterns after retraining of reaching movements with the MIME robotic system in subjects with post-stroke hemiparesis. *IEEE Transactions on Neural Systems and Rehabilitation Engineering*, 12, 186–194.

Mahoney, F. I., Barthel, D. W. (1965). Functional evaluation: the Barthel index. *Maryland State Medical Journal*, 14, 61-65.

Meng, W., Li, Q., Zhou Z., Ai, Q., Sheng, B., Xie S. (2015). Recent development of mechanisms and control strategies for robot-assisted lower limb rehabilitation. *Mechatronics*, 31,132-145.

Odugawa, V., Tiwari, A., Roy, R. (2005). Evolutionary computing in manufacturing industry: an overview of recent applications, Journal Applied Soft Computing, 5(3), 281-299.

Pittaccio, S., Viscuso, S. (2011). An EMG-controlled SMA device for the rehabilitation of the ankle joint in post-acute stroke. *Journal of Material Engineering and Performance*, 20, 666–670.

Preitl, S., Precup, R. E., Fodor, J., Bede, B. (2006), Iterative feedback tuning in fuzzy control systems. Theory and applications. *Acta Polytechnica Hungarica*, 3(3), 81-96.

Riener R., Luenenberger, L., Colombo, G. (2006). Human-centered robotics applied to gait training and assessment. *Journal of Rehabilitation Research and Development*, 43, 679–693.

Riener, R., Lunenburger, L., Jezernik, S., Anderschitz, M., Colombo, G., Dietz, V. (2005). Patient-cooperative strategies for robot-aided treadmill training: first experimental results. *IEEE Transactions on Neural Systems and Rehabilitation Engineering*, 13, 380–394.

Roy A, Krebs HI, Williams DJ, Bever CT, Forrester LW, Macko RM, Hogan, N. (2009). Robot aided neurorehabilitation: a novel robot for ankle rehabilitation. *IEEE Transactions on Robotics*, 25, 569-582.

Saglia, J. A., Tsagarakis, N. G., Dai, J. S., Caldwell, D. G. (2009). A high-performance redundantly actuated parallel mechanism for ankle rehabilitation. *International Journal of Robotic Research*,28, 1216–1227.

Saglia JA, Tsagarakis NG, Dai, J. S., Caldwell DG. (2012) Control strategies for patient assisted training using the ankle rehabilitation robot (ARBOT). *IEEE/ASME Transactions on Mechatronics*, 17(1), 1–10.

Shams, M., Rashedi, E., Dashti, S. M., Hakimi, A. (2017). Ideal gas optimization algorithm. International Journal of Artificial Intelligence, 15(2), 116-130.

Sheng, B., Zhang, Y., Meng, W., Deng, C., Xie, S. (2016). Bilateral robots for upper-limb stroke rehabilitation: State of the art and future prospects, *Medical Engineering and Physics*, 38, 587–606.

Simon, A. M., Brent Gillespie, R., Ferris D. P. (2007). Symmetry-based resistance as a novel means of lower limb rehabilitation. *Journal of Biomechanics*, 40, 1286–1292.

Song, R., Tong, K.-y., Hu, X., Li, L. (2008). Assistive control system using continuous myoelectric signal in robot-aided arm training for patients after stroke. *IEEE Transactions on Neural Systems and Rehabilitation Engineering*, 16, 371–379.

Song, R., Tong, K. Y., Hu, X. L., Zhou, W. (2013). Myoelectrically controlled wrist robot for stroke rehabilitation. *Journal of Neuroengineering and Rehabilitation*, 10:52.

Tóth, A., Arz, G., Fazekas. G., Bratanov, D., Zlatov, N. (2004). 25 Post-stroke shoulder-elbow physiotherapy with industrial robots. *Advances in Rehabilitation Robotics*. Springer, 391–411.

Vallery, H., van Asseldonk E. H. F., Buss, M., van der Kooij, H. (2009). Reference trajectory generation for rehabilitation robots: complementary limb motion estimation. *IEEE Transactions on Neural Systems and Rehabilitation Engineering*, 17, 23–30.

Volpe B. T., Krebs H. I., Hogan, N., Edelstein, L., Diels, C., Aisen, M. L. (2000) A novel approach to stroke rehabilitation: robot-aided sensorimotor stimulation. *Neurology*. 54, 1938-1944.

Veneman, J. F., Kruidhof, R., Hekman, E. E. G., Ekkelenkamp, R., Van Asseldonk E. H. F., van der Kooij, H. (2007). Design and evaluation of the LOPES exoskeleton robot for interactive gait rehabilitation. *IEEE Transactions on Neural Systems and Rehabilitation Engineering*, 15, 379–386.

Wolbrecht, E. T., Chan, V., Reinkensmeyer, D. J., Bobrow, J. E. (2008). Optimizing compliant model-based robotic assistance to promote neurorehabilitation. *IEEE Transactions on Neural Systems and Rehabilitation Engineering*, 16, 286–297.

Yin, Y. H., Fan, Y. J., Xu, L. D. (2012). EMG and EPP-integrated human-machine interface between the paralyzed and rehabilitation exoskeleton. *IEEE Transactions on Information Technology in Biomedicine*, 16, 542–549.